Quantifying the calibration uncertainty attributable to thermocouple inhomogeneity
Hill, Kenneth D.; Gee, Douglas J.

National Research Council Canada   Conseil national de recherches Canada

Canada

Quantifying The Calibration Uncertainty Attributable To Thermocouple Inhomogeneity

Kenneth D. Hill and Douglas J. Gee

National Research Council of Canada, Ottawa, Ontario, Canada

Abstract. Inhomogeneity in the Seebeck coefficient as a function of position along a thermocouple wire frequently dominates the uncertainty budgets of thermocouple calibration and use. The calibration process itself, simply through exposure to elevated temperatures for relatively modest times, generates both reversible and irreversible changes to the thermocouple that are a complex function of time, temperature, alloy composition, sheath structure, etc. We present data acquired using a salt bath at 250 °C to provide the step-function-like gradient that is our spatial probe of thermoelectric homogeneity. We show how the finite width of the step-function limits our ability to assess the "true" inhomogeneity of the thermocouple, and explore how the inhomogeneity impacts the calibration uncertainty attainable with the various thermal sources used for the calibration of thermocouples (based on their characteristic temperature gradients).

INTRODUCTION

Inhomogeneity in the Seebeck coefficient as a function of position along a thermocouple wire is a dominant component of thermocouple uncertainty budgets, and it remains a topic of ongoing interest within this symposium series [1-9] and beyond [10-23]. While manufacturers strive to deliver thermocouple wire that is as homogeneous as metallurgy and manufacturing processes allow, unavoidable degradations arise through use. The calibration process itself, simply through exposure to elevated temperatures for relatively modest times, generates both reversible and irreversible changes to the thermocouple that are a complex function of time, temperature, alloy composition, sheath structure, etc.

While our past practice has been to include in our thermocouple calibrations an uncertainty component for inhomogeneity based on a widely-accepted rule-of-thumb, the recent acquisition of a long-travel (300 mm) scanning stage allows us to scan thermocouples for inhomogeneity on a routine basis so that this important, and often dominant, uncertainty component can be based on measurements specific to the thermocouple under test.

The implementation of a thermocouple scanning capability tends to be unique to a particular laboratory. In our case, we have chosen to use a salt bath at 250 °C to provide the step-function-like gradient that is our spatial probe of thermoelectric homogeneity.

We present data acquired with this technique for a noble-metal with an analysis that demonstrates how the temperature gradient of the thermal source used in the calibration influences the component of uncertainty attributable to thermoelectric inhomogeneity.

FUNDAMENTALS

A brief review of thermocouple fundamentals may be helpful in understanding the analysis to be presented later. The voltage measured at the open ends of a pair of wires comprising conductor A and conductor B (each of length L) in a thermal gradient, and electrically connected to one another at $x=0$, is given by

$$E = \int_{x=0}^{L} S_{AB}(T, x) \cdot \left(\frac{dT}{dx}\right) \cdot dx \qquad (1)$$

where S_{AB} is the relative Seebeck coefficient of the pair of wires comprising the thermocouple. The dependence on both temperature ($T=T(x)$) and position along the wire (x) is explicit: the thermoelectric properties of the wires should not be considered homogeneous over their length. Inevitably, thermoelectric inhomogeneity arises from the spatial non-uniformity of both chemical (e.g. impurities, oxidation) and physical (e.g. dislocations, strain) influences, despite the best efforts of the manufacturers to deliver thermoelectrically uniform wire. Even when "new" wire approaches thermoelectric homogeneity, degradations arise during use and generally become more profound the higher the operating temperature.

It is clear from equation (1) that there is no contribution to the measured voltage from isothermal

portions of the wire (i.e. where the temperature gradient, dT/dx, is zero). It is also clear that if dT/dx were a delta-function at $x=x_0$, then equation (1) would become $E = S_{AB}(T(x_0), x_0)\times(T(L)-T(0))$ and such an ideal test gradient could be used to map the Seebeck coefficient along the wire. A delta-function is the derivative of a step-function, so a temperature source that maintains isothermal volumes at different temperatures on either side of a sharp interface is the real-world approximation to the ideal.

Even if an ideal step-function in temperature could be created, thermal conduction along the wire (and heat transfer limitations in general) precludes the realization of such spatially-detailed characterization. Realistic thermal conditions limit the characterization of the local Seebeck coefficient to spatial scales longer than the width of the thermal interface – just as a low-pass filter obscures signals beyond the cut-off frequency.

SCANNING FACILITY

Thermoelectric inhomogeneity scanning facilities can be divided into those with a single temperature gradient (i.e. a bath or furnace provides the hot zone) and those with two temperature gradients. The latter is often implemented with the thermocouple stationary and the heating zone movable. While moving heaters make it possible to scan thermocouples that are longer than a bath or furnace with limited immersion depth, the complexity of interpretation necessitated by the inclusion of a second gradient (and a corresponding second portion of voltage-generating wire) have led us to implement the single-gradient approach.

While the options for implementation are many, we have chosen a commercial salt bath operating at 250 °C as our normal characterization condition. The room-temperature air above the bath comprises the second zone. A commercial translation stage with 300 mm travel facilitates automated profiling by providing continuous motion at a defined speed, or step-wise motion through the programming of dwell periods at regular intervals. A fan sharpens the thermal interface and makes the profile more symmetric. Without the fan, the "tail" of the distribution for the in-air portion is extended and the indicated temperature remains significantly above that of the surrounding air ($\Delta T \sim 10$ to 15 °C).

To characterize the temperature gradient, a special Type-S thermocouple with the junction 29 cm from the end of the twin-bore alumina tube (the Pt wire loops around the open end of the tube) was used to obtain the data of Figure 1. The derivative of the temperature gradient resembles a Gaussian, but the

asymmetry is better-represented by the sum of two Gaussians:

$$\frac{dT}{dx} = a_1 \exp\left(-\left(\frac{x-b_1}{c_1}\right)^2\right) + a_2 \exp\left(-\left(\frac{x-b_2}{c_2}\right)^2\right) \qquad (2)$$
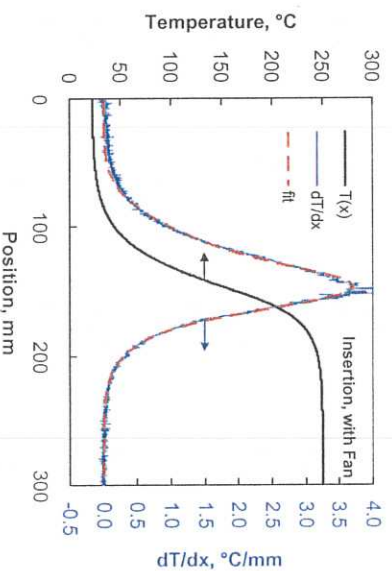

Figure 1. The temperature profile obtained when inserting the specially-constructed test thermocouple into the salt bath. Its derivative (blue curve, right axis), and the two-Gaussian fit to the derivative (red curve, right axis) are also shown.

SOURCE CHARACTERISTICS

Because the voltage measured during a calibration arises from the convolution of the Seebeck coefficient of the thermocouple with the temperature gradient, the uncertainty component attributable to inhomogeneity depends on the temperature gradient (dT/dx) of each source (furnace or bath) that contributes data to the calibration. Figure 2 shows the axial temperature profiles of some of the baths and furnaces employed.

The gradients of the thermal sources can be obtained by numerically differentiating the immersion profiles. From Figure 3, it is evident that the gradients differ significantly from one another, with some nearly Gaussian and others significantly asymmetric. Not surprisingly, the sources that are higher in temperature have larger peak values of dT/dx. In an effort to quantify the spatial extent over which the Seebeck coefficient is averaged with each source, the full width at half maximum (FWHM) has been evaluated (see Table 1). By comparing the FWHM of the various sources, it is evident that the Ag fixed point and the tube furnace (at 980 °C) probe the thermal homogeneity at spatial scales shorter than those accessible via the salt bath.
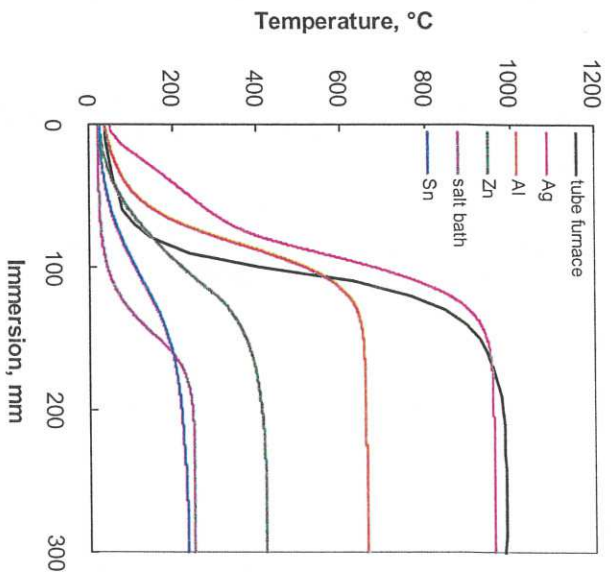
Temperature, °C

Figure 2. The immersion profiles of various thermal sources used for the calibration of thermocouples at NRC. The tube furnace temperature is at 980 °C and the salt bath at 250 °C.
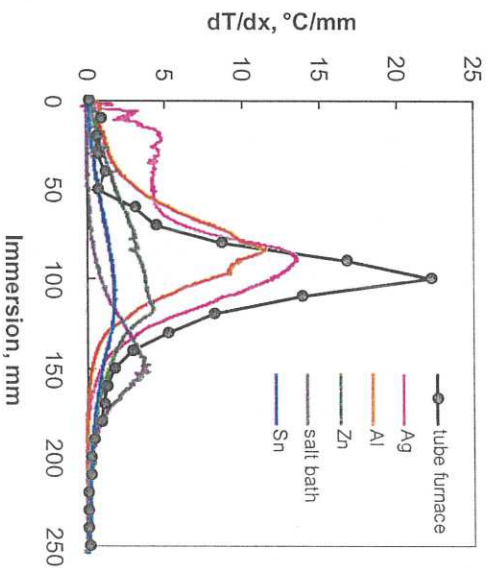
dT/dx, °C/mm

Immersion, mm

Figure 3. The numerical derivative of Figure 2.

TABLE 1. Peak height and full width at half maximum of the temperature gradients (dT/dx) of the thermal sources shown in Figure 3.

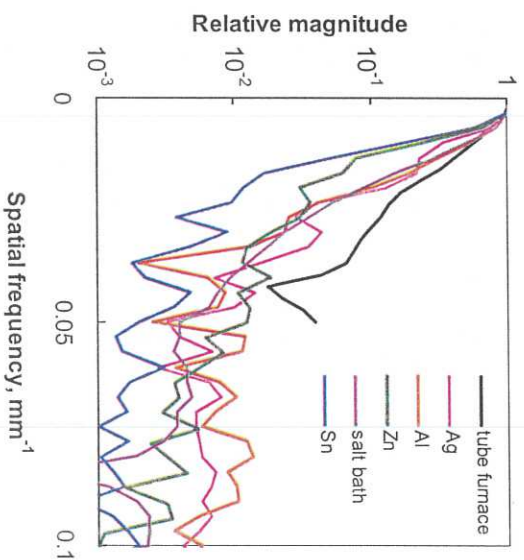| Source	Max. dT/dx (°C/mm)	FWHM (mm)
Ag fixed point	13.7	27.7
Al fixed point	11.5	46.1
Zn fixed point	4.27	81.4
Sn fixed point	1.81	99.1
tube furnace (980 °C)	22.5	29.4
salt bath (250 °C)	3.70	50.7

Relative magnitude

Spatial frequency, mm^{-1}

Figure 4. Fourier transform of the data from Figure 3, normalized to the maximum value to facilitate comparison.

In the spatial frequency domain (Figure 4), the response of the tube furnace extends to higher frequencies than that of the salt bath. The responses of the Al and Ag fixed points appear comparable to that of the salt bath. As each source is analogous to a low-pass filter, we must assume that the intrinsic inhomogeneity is greater than the measurements indicate, and that the observable inhomogeneity will be larger for sources with sharper gradients (i.e. higher frequency response).

SIMULATIONS

Simulations were employed to obtain insight into the signals arising from the scanning process. Our simulated temperature profile has the shape of the error function, but scaled and offset.

$$T(x) = a \times \left(1 + erf\left(\frac{x-b}{c}\right)\right) + d \quad (3)$$

The values $a = 113.75$ °C, $b = 141$ mm, $c = 39$ mm, and $d = 22.5$ °C were used to approximate the immersion profile of the salt bath. Figure 5 compares the simulated profile to the measured one, and also shows the derivative, dT/dx. The full width at half maximum (FWHM) of dT/dx is approximately equal to 1.66c. The simulated values compare well with Figure 1.

The Seebeck coefficient was approximated by a constant plus a 1% sinusoidal variation, with f the number of cycles per 300 mm.

$$S(x) = 10 + 0.1\sin\left(\frac{2\pi x f}{300}\right) \qquad (4)$$

The goal was to explore the attenuation of variations in the Seebeck coefficient by the finite width of the thermal interface, as represented by the parameter c in equation (3).
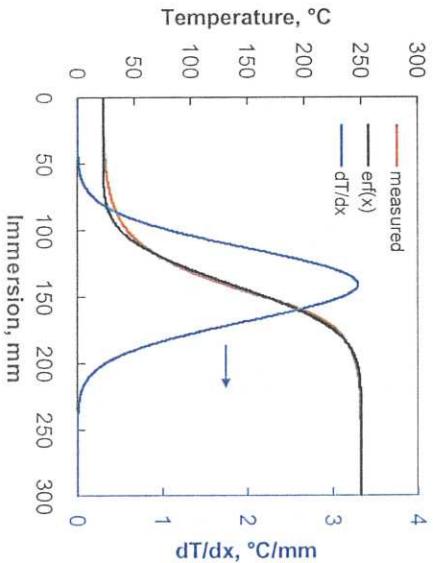

Figure 5. The temperature profile described by equation (3). Its derivative (blue curve, right axis) is a Gaussian. The red curve is the measured profile of the salt bath.

The simulation was used to test the analysis methodology. To that end, we started with the temperature profile of equation (3), computed the numerical derivative, and then its Fourier transform, $T(k)$. Then we calculated the Fourier transform of the Seebeck coefficient, $S(k)$, multiplied $T(k)$ by $S(k)$ to form $E(k)$, and took the inverse Fourier transform, $E(x)$. This is the quantity that corresponds to the signal measured during a scan. With the simulation, we were able to explore how the c parameter in equation (3) and f in equation (4) influence the amplitude of the oscillations in $E(x)$. The results are presented in Figures 6 and 7. While the gradient of the tube furnace is less well-modeled by equation (3) than the salt bath, its maximum slope is reasonably approximated when $c = 30$ mm.

The frequency response can be computed via Fourier transform (Figure 8) and compared with the experimentally-derived values (Figure 4). The experimental frequency responses roll off much less rapidly than the simulation, suggesting either that equation (3) is an inadequate representation of the shape of the thermal gradient or that the experimental data is contaminated by noise.
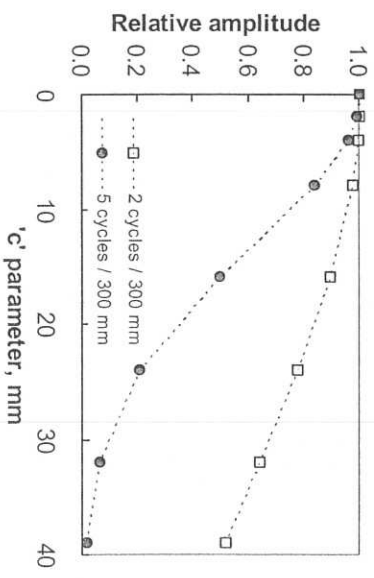

Figure 6. The variation in the amplitude of the oscillations in $E(x)$ as a function of the width of the thermal interface, as represented by the c parameter.
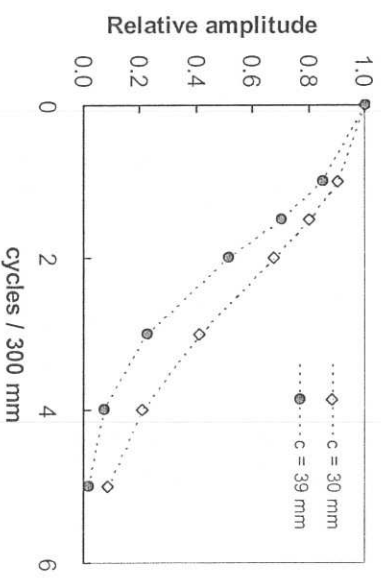

Figure 7. The variation in the amplitude of the oscillations in $E(x)$ as a function of their frequency.
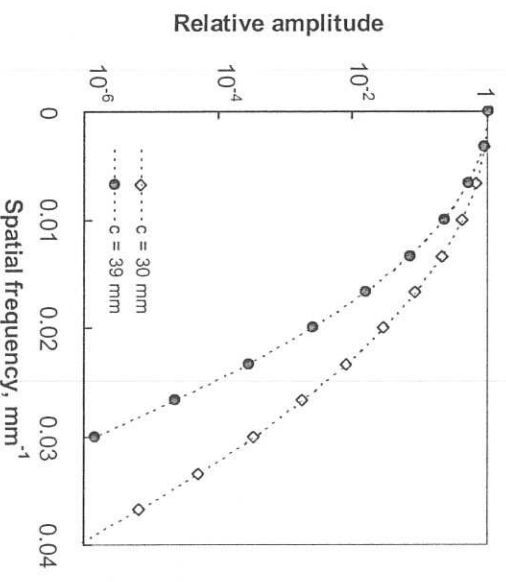

Figure 8. The spatial frequency response of equation (3).

REPRESENTATIVE SCANS

Figures 9 is an example of data obtained with our scanning apparatus for a Type-S thermocouple. Availability of the scanning capability has allowed us to track changes in the inhomogeneity at various stages of the calibration process: as-received, after annealing, and following the calibration. The maximum and minimum values observed can be used to estimate the uncertainty component for inhomogeneity.
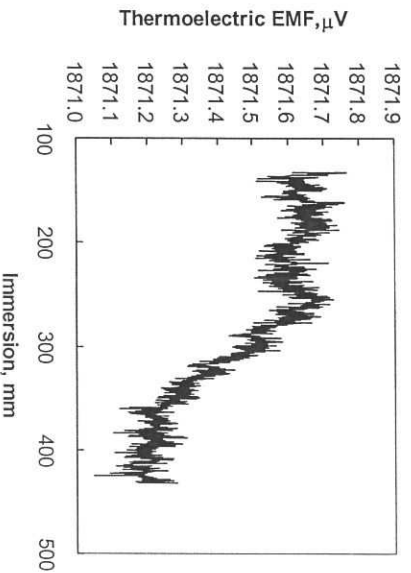

Figure 9. The variation in the temperature indicated by a type-S thermocouple as a function of immersion depth into the salt bath used to probe thermoelectric inhomogeneity.

CALIBRATION UNCERTAINTY

The goal of this study was to quantify the calibration uncertainty attributable to thermoelectric inhomogeneity. The simplest approach is to assume that the relative variation in the measured voltage, $\Delta E/E$, remains constant for all temperatures and calibration sources. However, the width of the thermal interface of the salt bath acts like a low-pass spatial filter, attenuating the higher-frequency components. Thermal sources with temperature gradients of greater width than that of the salt bath (e.g: Zn fixed point) can be expected to exhibit lower values of $\Delta E/E$ while those with narrower gradients (e.g. tube furnace at 980 °C) should have higher values of $\Delta E/E$ – but by how much?

Our approach is to collect the scan data ($E(x)$), compute its Fourier transform ($E(k)$), and divide by the Fourier transform of the gradient of the salt bath ($T'(k)$) to obtain $S(k)$, a quantity indicative of the "true" thermoelectric inhomogeneity. Then, $S(k)$ is multiplied by the Fourier transform of the gradient of the particular bath or furnace used for the calibration, and an inverse Fourier transform produces $E_c(x)$ for that calibration source. The variation $\Delta E_c/E_c$ is the measure

---

of the thermoelectric inhomogeneity (for the calibration).

In practice, a cut-off frequency is employed when multiplying the Fourier transform of the measured signal, $E(k)$, by the ratio $(T_{TF}(k)) / (T_{SB}(k))$ ('TF' is the tube furnace and 'SB' is the salt bath) to minimize the amplification of noise. This cut-off is typically 0.04 mm^{-1}, but operator judgment is required to ensure the output is a likely representation. Filtering in the frequency domain may also be employed to reduce the high-frequency noise. Figure 10 is the result of this Fourier transform-based analysis of the data from Figure 9, to estimate the thermoelectric inhomogeneity anticipated from the tube furnace. The transients at the beginning and end are an artifact of the analysis and are ignored in estimating the relative uncertainty, ur.

$$u_r = \frac{(E_{max} - E_{min})}{(E_{max} + E_{min})} \times \frac{1}{\sqrt{3}} \tag{5}$$
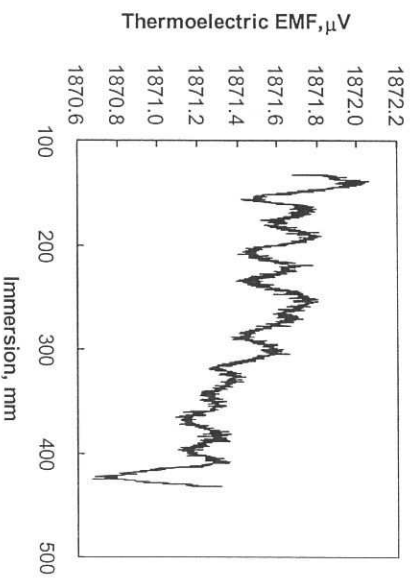

Figure 10. The same data as in Figure 9 but processed via Fourier transforms to approximate the response expected in the thermal gradient of the tube furnace.

CONCLUSIONS

We have explored a methodology to estimate the impact of thermoelectric inhomogeneity on the uncertainty of the calibration process. The finite width of the thermal gradient of the salt bath acts like a spatial low-pass filter that attenuates the higher-frequency components. The calibration uncertainty attributable to thermoelectric inhomogeneity will be less than the value derived from the salt bath data for thermal profiles with a broader spatial extent (as represented by the FWHM of their gradient, dT/dx). In this case, a conservative estimate of the inhomogeneity component can be derived by directly using the $\Delta E/E$ value measured using the salt bath. The more challenging case is when the calibration source has a

gradient of narrower spatial extent relative to that of the salt bath. In this case, use of the salt bath-derived value would lead to an underestimate of the uncertainty component so the higher-frequency components contributing to the estimate require enhancement. However, as Ballico [17] has remarked, the methodology is challenging to implement in practice due to differences in transfer functions among thermocouples, noise in determining the thermal gradients, and difficulty in maintaining reproducible thermal conditions between the time that the 'reference' profile is obtained and the time that the thermocouple under test is scanned.

REFERENCES

1. Carr, K. R., "Testing of Ceramic Insulator Compaction and Thermoelectric Inhomogeneity in Sheathed Thermocouples" in *Temperature, Its Measurement and Control in Science and Industry*, Vol. 4, edited by D. I. Finch, G. W. Burns, R. L. Berger and T. E. Van Zandt, Pittsburgh: Instrument Society of America, 1972, pp. 1855-1868.

2. Fenton, A. W., "The Traveling Gradient Approach to Thermocouple Research" in *Temperature, Its Measurement and Control in Science and Industry*, Vol. 4, edited by D. I. Finch, G. W. Burns, R. L. Berger and T. E. Van Zandt, Pittsburgh: Instrument Society of America, 1972, pp. 1973-1990.

3. Mossman, C. A., Horton, J. L. and Anderson, R. L., "Testing of thermocouples for inhomogeneities: A review of theory, with examples" in *Temperature, Its Measurement and Control in Science and Industry*, Vol. 5, edited by J. F. Schooley, New York: American Institute of Physics, 1982, pp. 923-930.

4. Reed, R. P., "Thermoelectric inhomogeneity testing: Part I – Principles" in *Temperature, Its Measurement and Control in Science and Industry*, Vol. 6, edited by J. F. Schooley, New York: American Institute of Physics, 1992, pp. 519-524.

5. Reed, R. P., "Thermoelectric inhomogeneity testing: Part II – advanced methods" in *Temperature, Its Measurement and Control in Science and Industry*, Vol. 6, edited by J. F. Schooley, New York: American Institute of Physics, 1992, pp. 525-530.

6. Jahan, F. and Ballico, M., "A Study of the Temperature Dependence of Inhomogeneity in Platinum-Based Thermocouples" in *Temperature, Its Measurement and Control in Science and Industry*, Vol. 7, edited by D. C. Ripple, AIP Conference Proceedings 684, New York: American Institute of Physics, 2002, pp. 469-474.

7. Gotoh, M., "Thermoelectric scanning Study of Pt/Pd and Au/Pt Thermocouples up to 960 °C with a Pressure Controlled sodium Heat-Pipe" in *Temperature, Its Measurement and Control in Science and Industry*, Vol. 7, edited by D. C. Ripple, AIP Conference Proceedings 684, New York: American Institute of Physics, 2002, pp. 481-484.

8. Reed, R. P., "The effect of Interrogating Temperature profile in the Seebeck Inhomogeneity Method of test

9. Zvizdic, D., Serfezi, D., Bermanec, L. G., Bonnier, G. and Renaot, E., "Estimation of Uncertainties in Comparison Calibration of Thermocouples" in *Temperature, Its Measurement and Control in Science and Industry*, Vol. 7, edited by D. C. Ripple, AIP Conference Proceedings 684, New York: American Institute of Physics, 2002, pp. 529-534.

10. Kollie, T. G., Horton, J. L., Carr, K. R., Herskovitz, M. B. and Mossman, C. A., *Rev. Sci. Instrum.* **46**, 1447-1461 (1975).

11. Bentley, R. E., *Meas. Sci. Technol.* **11**, 538-546 (2000).

12. Ogura, H., Tamba, J., Izuchi, M. and Arai, M., "Effect of Temperature Distribution on Emf of Thermocouples" in *Proceedings of SICE 2002 Annual Conference*, Tokyo: Society of Instrument and Control Engineers, 2002, pp. 498-500.

13. Gotoh, M., "Study of the Immersion Characteristic of Thermocouples with a Heat-pipe up to 960 °C" in *Proceedings of SICE 2002 Annual Conference*, Tokyo: Society of Instrument and Control Engineers, 2003, pp. 744-748.

14. Ogura, H., Numajiri, H., Izuchi, M. and Arai, M., "Evaluation of Inhomogeneity of Pt/Pd Thermocouples" in *Proceedings of SICE 2003 Annual Conference*, Tokyo: Society of Instrument and Control Engineers, 2003, pp. 503-506.

15. Ogura, H., Numajiri, H., Izuchi, M. and Arai, M., "Evaluation of Inhomogeneity of Pt/Pd Thermocouples" in *Proceedings of SICE 2003 Annual Conference*, Tokyo: Society of Instrument and Control Engineers, 2003, pp. 744-748.

16. Liedberg, H., "Thermoelectric homogeneity of metal-sheathed type K thermocouples" in *TEMPMEKO 2004, 9th International Symposium on Temperature and Thermal Measurements in Industry and Science*, Vol. 1, edited by D. Zvizdic, Zagreb: LPM/FSB, 2005, pp. 453-464.

17. Ballico, M., "Numerical post-correction of thermocouple inhomogeneity scan data to improve spatial resolution and reduce conduction errors" in *TEMPMEKO 2004, 9th International Symposium on Temperature and Thermal Measurements in Industry and Science*, Vol. 2, edited by D. Zvizdic, Zagreb: LPM/FSB, 2005, pp. 801-806.

18. Pearce, J. V., *Meas. Sci. Technol.* **18**, 3489-3495 (2007).

19. Holmsten, M., Ivarsson, M., Falk, R., Lidbeck, M. and Josefson, L-E., *Int. J. Thermophys.* **29**, 915-925 (2008).

20. Abdelaziz, Y. A. and Edler, F., *Meas. Sci. Technol.* **20**, 055102 (9 p.) (2009).

21. Kim, Y-G., Song, C. H., Gam, K. S. and Yang, I., *Meas. Sci. Technol.* **20**, 075102 (5 p.) (2009).

22. White, D. R. and Mason, R. S., *Int. J. Thermophys.* **31**, 1654-1662 (2010).

23. Tamba, J., Yamazawa, K., Masuyama, S., Ogura, H. and Izuchi, M. *Int. J. Thermophys.* **32**, 2436-2451 (2011).